THE UNLOADING COMPLIANCE PROCEDURE FOR *J-R* CURVE TESTING USING SE(T) FRACTURE SPECIMENS

Sebastian Cravero, scravero@gmail.com
Mario Sérgio Giancoli Chiodo, mario.sg@gmail.com
Claudio Ruggieri, claudio.ruggieri@poli.usp.br
Department of Naval Architecture and Ocean Engineering, PNV-EPUSP
University of São Paulo, São Paulo, SP 05508–900, Brazil

Abstract *– This work provides an estimation procedure to determine J-resistance curves for SE(T) fracture specimens using the unloading compliance technique and the eta-method. Collaborative experimental and computational investigations now underway exploit these methods support development of a standard test procedure for this crack configuration. In the present study, attention is directed to pin-loaded SE(T) specimens with varying geometry and crack sizes but representative solutions are also included for clamped SE(T) specimens. A summary of the methodology upon which J and* Δa *are derived sets the necessary framework to determine crack resistance data from the measured load* vs. *displacement curves. The extensive plane-strain analyses enable numerical estimates of the nondimensional compliance,* μ*, and the plastic factors* η *and* γ *for a wide range of specimen geometries and material properties characteristic of structural and pipeline steels. The results presented here produce a representative set of solutions which lend further support to develop standard test procedures for constraint-designed SE(T) specimens applicable in measurements of crack growth resistance for pipelines.*

Keywords*: resistance curves, ductile fracture, unloading compliance, SE(T) specimen, eta-factor*

1. INTRODUCTION

Safety analyses and engineering critical assessments (ECA) of damaged pipelines remain a key issue in design and operation of high pressure piping systems, including onshore and offshore facilities. As the pipeline infrastructure ages, robust procedures for integrity analyses become central to specifying critical flaw sizes which enter directly into procedures for repair decisions and life-extension programs of in-service structural components. Perhaps more importantly, these procedures must ensure fail-safe operations which avoid costly leaks and ruptures due to material failure to comply with the current stringent environment-based regulations. Current codes and standards for oil and gas pipelines provide rules for welding, inspection and testing of transmission pipelines (see, for example, API 1104 (1999), CSA Z662 (1999)). While these codes provide simplified acceptance criteria for fabrication defects (such as slag inclusions and porosity in weldments) based upon workmanship standards and fracture toughness testing, they not specifically address stable ductile tearing of crack-like defects that form during in-service operation.

Many structural steels generally exhibit significant increases in fracture toughness, characterized by the J Integral (Rice, 1968), over the first few mm of stable crack extension (Δa), often accompanied by large increases in background plastic deformation. Conventional testing programs to measure crack growth resistance (J-Δa) curves routinely employ three-point bend, SE(B), or compact, C(T), specimens containing deep, through cracks ($a/W \geq 0.5$). However, laboratory testing of fracture specimens to measure resistance curves (also often termed R-curves) consistently reveals a marked effect of absolute specimen size, geometry, relative crack size (a/W) and loading mode (tension *vs*. bending) on toughness at similar amounts of crack growth (see Joyce and Link (1995) for representative experimental studies). These effects observed in R-curves have enormous practical implications in defect assessments and repair decisions of in-service structures under low constraint conditions. Structural components falling into this category include pressurized piping systems with surface flaws that form during fabrication or during in-service operation (e.g., weld cracks and cracks derived from blunt corrosion, slag and nonmetallic inclusions, dents at weld seams, etc.) (Eiber and Kiefner, 1986; AWS, 1987; NEB, 1996). These crack configurations generally develop low levels of crack-tip stress triaxiality (associated with the predominant tensile loading which develops in pressurized piping systems) thereby contrasting sharply to conditions present in deeply cracked SE(B) and C(T) specimens. Consequently, defect assessments of cracked pipelines based on standard, deep notch specimens may be unduly conservative and overly pessimistic. While such conservatism represents an extra factor of safety, excessive pessimism in defect assessments can lead to unwarranted repairs or replacement of in-service pipelines at great operational costs.

These observations have prompted research efforts to support the use of geometry dependent fracture toughness values in defect assessment procedures for structural components under low constraint conditions. Specifically for pressurized pipelines and cylindrical vessels, there has recently been a surge of interest in predicting fracture behavior based upon single edge notch tension specimens – SE(T)[†] (see, e.g., Nyhus (1999) and Nyhus and Ostby (2002)). The primary motivation to use SE(T) fracture specimens in defect assessment procedures of cracked pipes is the strong similarity in crack-tip stress and strain fields which drive the fracture process for both crack configurations (Cravero and Ruggieri, 2005). These previous research initiatives represent a significant promise in engineering applications of constraint-designed SE(T) fracture specimens. However, full understanding of the fracture behavior directly connected to this crack configuration which supports development of standard test procedures is still lacking.

As a step in this direction, this work provides an estimation procedure to determine J-resistance curves for SE(T) fracture specimens using the unloading compliance technique and the *eta*-method. Collaborative experimental and computational investigations now underway exploit these procedures to support development of a standard test procedure for this crack configuration. In the present study, attention is directed to pin-loaded SE(T) specimens with varying geometry and crack sizes but representative solutions are also included for clamped SE(T) specimens. A summary of the methodology upon which J and Δa are derived sets the necessary framework to determine crack resistance data from the measured load *vs.* displacement curves. The extensive plane-strain analyses enable numerical estimates of the nondimensional compliance, μ, and the plastic factors η and γ for a wide range of specimen geometries and material properties characteristic of structural and pipeline steels. The results presented here produce a representative set of solutions which lend further support to develop standard test procedures for constraint-designed SE(T) specimens applicable in measurements of crack growth resistance for pipelines.

2. ESTIMATION PROCEDURE OF *J-R* CURVES

Analytical efforts to support the development of laboratory measurements for fracture toughness resistance data have focused primarily on the unloading compliance method based upon testing of a single specimen. Implementation of the method essentially follows from determining the instantaneous value of J and specimen compliance at partial unloading during the measurement of the load-displacement curve as illustrated in Fig. 1(a). The technique then enables accurate estimations of J and Δa at several locations on the load-displacement records from which the J-R curve can be developed. Before deriving the quantities and parameters needed to determine the crack growth resistance curves for the SE(T) specimens, this section first provides an overview on the nature of the methodology.

The procedure to estimate crack growth resistance data begins by invoking the energy release rate interpretation of the J-integral. Upon consideration of the elastic and plastic contributions to the strain energy for a cracked body under Mode I deformation (Anderson, 2005), J can be conveniently defined in terms of its elastic component, J_{el}, and plastic component, J_{pl}, as

$$J = J_{el} + J_{pl} = \frac{K_I^2}{E'} + \frac{\eta_J A_{pl}}{B_N b_0} \tag{1}$$

where K_I is the elastic stress intensity factor for the cracked configuration, A_{pl} is the plastic area under the load-displacement curve, B_N is the net specimen thickness at the side groove roots ($B_N = B$ if the specimen has no side grooves where B is the specimen gross thickness), b_0 is the initial uncracked ligament ($b_0 = W - a_0$ where W is the width of the cracked configuration and a_0 is the initial crack length). In writing the first term of Eq. (1), plane-strain conditions are adopted such that $E' = E/(1-\nu^2)$ where E and ν are the (longitudinal) elastic modulus and Poisson's ratio, respectively. Factor η_J introduced by Sumpter and Turner (1976) represents a nondimensional parameter which relates the plastic contribution to the strain energy for the cracked body and J. Fig. 1(b) illustrates the essential features of the estimation procedure for J_{pl}. Here, we note that A_{pl} (and consequently η_J) can be defined in terms of load-load line displacement (*LLD* or Δ) data or load-crack mouth opening displacement (*CMOD* or V) data. For definiteness, these quantities are denoted η_J^{CMOD} and η_J^{LLD}. While both definitions serve essentially as a means to quantify the effect of plastic work on the J-integral, η_J-values based on *LLD* have a different character than the corresponding η_J-values based on *CMOD*. This issue is discussed in more details in the next sections.

The previous expression (1) defines the key quantities driving the evaluation procedure for J as a function of applied (remote) loading and crack size. Further, the previous solution for J_{pl} retains strong contact with the deformation plasticity definition of J and thus assumes nonlinear elastic material response. However, the area under the actual load-displacement curve for a growing crack differs significantly from the corresponding area for a stationary crack (which the deformation

---

[†)] This specimen is also denoted SENT in the European literature.

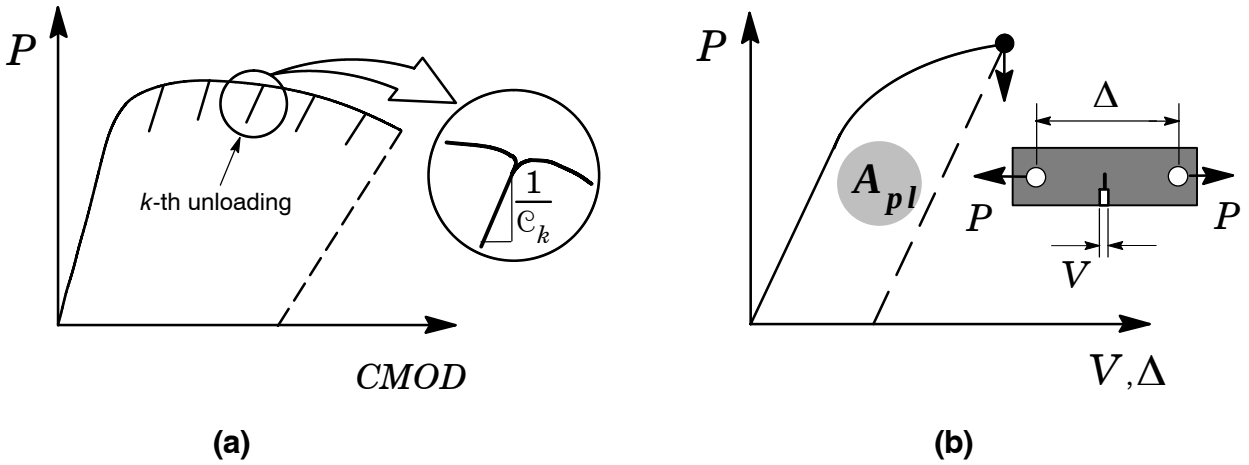

Figure 1 *(a) Partial unloading during the evolution of load with crack mouth opening displacement; (b) Definition of the plastic area under the load-displacement curve.*

definition of J is based on) (Anderson, 2005). Consequently, the measured load-displacement records must be corrected for crack extension to obtain an accurate estimate of J-values with increased crack growth. A widely used approach (which forms the basis of current standards such as ASTM E1820 (2001)) to evaluate J with crack extension follows from an incremental procedure which updates J_{el} and J_{pl} at each partial unloading point, denoted k, during the measurement of the load *vs.* displacement curve in the form

$$J_k = J_{el}^k + J_{pl}^k \quad . \tag{2}$$

Within this approach, the k-th elastic term of J is directly calculated from the corresponding k-th value of K_{I} using the first term of previous Eq. (1) which yields

$$J_{el}^K = \frac{\left(K_{\mathrm{I}}^k\right)^2}{E'} \quad . \tag{3}$$

For the SE(T) specimen, parameter K_{I} is evaluated at the current load, P_k, as

$$K_{\mathrm{I}}^k = \frac{P_k}{B_N\sqrt{W}}\,\mathcal{F}\left(a_k/W\right) \tag{4}$$

where $\mathcal{F}\left(a_k/W\right)$ defines a nondimensional stress intensity factor dependent upon specimen geometry, crack size and loading condition. The Appendix provides analytical expressions for the nondimensional stress intensity factors $\mathcal{F}\left(a_k/W\right)$ for the SE(T) specimens analyzed here, .

Similarly, the k-th plastic term of J follows from the second term of Eq. (1) using the current plastic area, A_{pl}^k. Given an estimated value for J_{pl} at $k-1$, the k-th value of J is given by

$$J_{pl}^k = \left[J_{pl}^{k-1} + \frac{\eta_{k-1}}{b_{k-1}B_N}\left(A_{pl}^k - A_{pl}^{k-1}\right)\right] \times \Gamma \tag{5}$$

in which Γ is defined as

$$\Gamma = 1 - \frac{\gamma_{k-1}}{b_{k-1}}\left(a_k - a_{k-1}\right) \tag{6}$$

where factor γ is evaluated from

$$\gamma_{k-1} = \left[-1 + \eta_{k-1} - \left(\frac{b_{k-1}}{W}\frac{\eta'_{k-1}}{\eta_{k-1}}\right)\right] \tag{7}$$

with

$$\eta'_{k-1} = W\frac{d\eta_{k-1}}{da_{k-1}} \quad . \tag{8}$$

Another key step in the experimental evaluation of crack growth resistance response involves the accurate estimation of the instantaneous crack length as testing progresses. The unloading compliance technique provides a convenient and yet simple procedure to correlate crack extension to the specimen compliance with increased crack growth. Fig. 1(a) illustrates the essential features of the method. The slope of the load-displacement curve during the *k*-th unloading defines the instantaneous specimen compliance, denoted $\mathbb{C}_k$, which depends on specimen geometry and crack length.

Application of the procedure outlined above requires correct specification of all quantities entering directly into the calculation of *J* through Eq. (2-8) as well as the specimen compliance, $\mathbb{C}$. These quantities thus play a crucial role in defining the *J-R* curve from laboratory measurements of load *vs.* displacement for the tested specimen. Current test standards provide appropriate forms for factors η, γ and the compliance $\mathbb{C}$ which are only applicable to C(T) and SE(B) specimens with deep cracks ($a/W \geq 0.45$). The relatively limited analyses and data available to construct crack growth resistance data for SE(T) specimens underscores the need for improved and accurate descriptions of factors η, γ and compliance $\mathbb{C}$ for these crack configurations. The following sections explore detailed numerical and validation analyses which lead to a definite set of expressions describing those key quantities.

3. NUMERICAL PROCEDURES

3.1 Finite Element Models

Detailed finite element analyses are performed on plane-strain models for a wide range of 1-T SE(T) specimens (thickness $B = 25.4$ mm). The analysis matrix includes specimens with $a/W = 0.1$ to 0.7 with increments of 0.1, and $H/W = 4$, 6 and 10. Here, *a* is the crack size specimen, *W* is the specimen width and *H* is the distance between the pin loading or clamps. The analyses also consider the effect of loading conditions, pin-loaded ends *vs.* clamped ends; these specimens are denoted as $SE(T)_P$ and $SE(T)_C$. Figures 2(a-b) shows the geometry and specimen dimensions for the analyzed crack configurations.

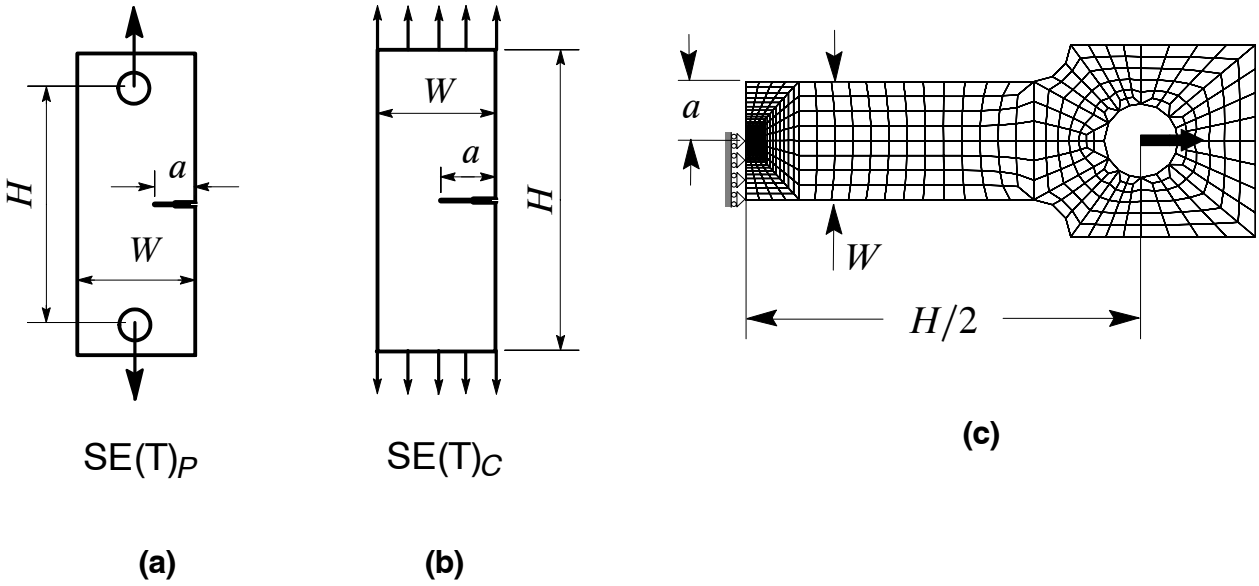

Figure 2 *Geometries for analyzed SET fracture specimens: (a) Pin-loaded specimens; (b) Clamped specimens; (c) Finite element model used in plane-strain analyses of the pin-loaded SE(T) specimen with a/W = 0.5 and H/W=6.*

Figure 2(c) shows the finite element model constructed for the plane-strain analyses of the pin-loaded SE(T) specimen with $a/W = 0.5$ and $H/W = 6$. All other crack models have very similar features. A conventional mesh configuration having a focused ring of elements surrounding the crack front is used with a small key-hole at the crack tip. Our previous numerical analyses (Cravero and Ruggieri, 2005) reveal that such mesh design provides detailed resolution of the near-tip stress-strain

fields thereby providing accurate numerical evaluation of J-values. Symmetry conditions permit modeling of only one-half of the specimen with appropriate constraints imposed on the remaining ligament. A typical half-symmetric model has one thickness layer of 1365 8-node, 3-D elements (2950 nodes) with plane-strain constraints imposed on each node.

3.2 Computational Procedure and Material Laws

The finite element code WARP3D (Koppenhoefer, 1994) provides the numerical solutions for the plane-strain analyses reported here. The code enables conventional linear elastic analysis and incorporates both a Mises (J_2) constitutive model in both small-strain and finite-strain framework. Evaluation of the J-integral derives from a domain integral procedure (Moran and Shih, 1987) which yields J-values in excellent agreement with estimation schemes based upon *eta*-factors for deformation plasticity (ASTM E1820, 2001) while, at the same time, retaining strong path independence for domains defined outside the highly strained material near the crack tip.

To construct the relationship between specimen compliance, $\mathbb{C}$, and crack length, a series of linear elastic analyses provides the load-displacement ratios for all fracture models. These analyses adopt conventional values for the elastic constants, $E = 206$ GPa and $\nu = 0.3$. Evaluation of factors η and γ requires nonlinear finite element solutions which include the effects of plastic work on J and the load-displacement response. These analyses utilize an elastic-plastic constitutive model with J_2 flow theory and conventional Mises plasticity in small geometry change (SGC) setting. The numerical solutions employ a simple power-hardening model to characterize the uniaxial true stress ($\bar{\sigma}$) *vs.* logarithmic strain (ϵ) in the form

$$\frac{\epsilon}{\epsilon_0} = \frac{\bar{\sigma}}{\sigma_0} \quad \epsilon \le \epsilon_0 \; ; \qquad \frac{\epsilon}{\epsilon_0} = \left(\frac{\bar{\sigma}}{\sigma_0}\right)^n \quad \epsilon > \epsilon_0 \tag{9}$$

where σ_0 and ϵ_0 are the reference (yield) stress and strain, and n is the strain hardening exponent. The finite element analyses consider material flow properties covering typical pipeline grade steels with $E = 206$ GPa and $\nu = 0.3$: $n = 5$ and $E/\sigma_0 = 800$ (high hardening material), $n = 10$ and $E/\sigma_0 = 500$ (moderate hardening material), $n = 20$ and $E/\sigma_0 = 300$ (low hardening material). These ranges of properties also reflect the upward trend in yield stress with the decrease in strain hardening exponent characteristic of ferritic pipeline steels.

4. RESULTS AND DISCUSSION

The following sections provide selected key results for the extensive numerical analyses conducted for pin-loaded and clamped SE(T) specimens with varying configurations. These results include compliance equations and factors η and γ needed to determine Δa and J from experimentally measured load-displacement records. The analyses also explore the effect of the estimation scheme (*CMOD vs. LLD*) on plastic *eta*-factors for pin-loaded SE(T) specimens.

4.1 Compliance Equations

Standard elastic analyses under plane-strain conditions typically define the (linear) dependence of applied load on displacement for a given specimen geometry with different crack sizes. Such dependence provides the required data from which the specimen compliance for varying crack size is extracted. By performing a series of finite element analyses for other specimen geometries, determination of $\mathbb{C}$ proceeds as previously described. Figures 3(a-b) provide the variation of normalized compliance, μ, with crack length to specimen width ratio, a/W, for the pin-loaded and clamped SE(T) specimens with varying H/W-ratios. In all plots, the normalized compliance μ is defined by (Saxena, 1998)

$$\mu = \frac{1}{1 + \sqrt{E' B_{ef} \mathbb{C}}} \tag{10}$$

where

$$B_{ef} = B - \frac{\left(B - B_N\right)^2}{B} \quad . \tag{11}$$

The results displayed in Fig. 3(a) reveal that the compliance μ for the pin-loaded SE(T) specimen is essentially independent of specimen length as characterized by the H/W-ratio; here, all curves collapse onto a single curve defining the dependence of μ on a/W. For the clamped SE(T) specimens, the results displayed in Fig. 3(b) exhibit a rather different behavior in which the compliance μ depends on the H/W-ratio for deeper cracks ($a/W \gtrsim 0.4$); however, μ is essentially independent of H/W for shallow cracks ($a/W \lesssim 0.2$).

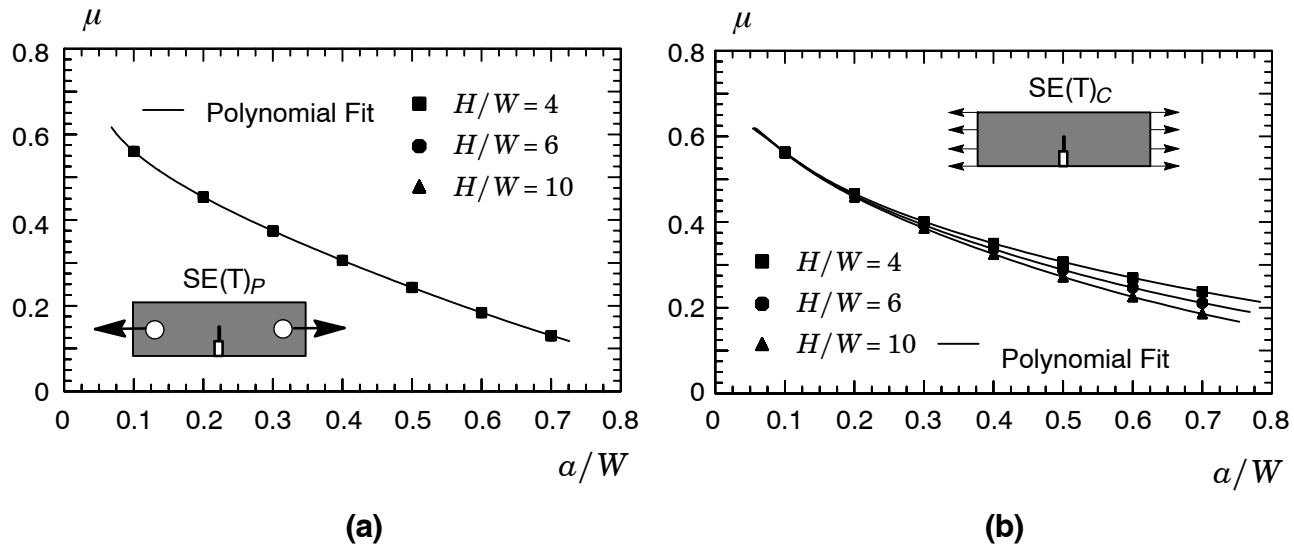

Figure 3 *Variation of compliance, μ, with a/W-ratio: a) pin-loaded SE(T) specimens with different H/W-ratios; b) clamped SE(T) specimens with different H/W-ratios..*

Using now the previous results for guidance, we construct the functional dependence of crack length and specimen compliance as follows:

$$\frac{a}{W} = c_0 + c_1\mu + c_2\mu^2 + c_3\mu^3 + c_4\mu^4 + c_5\mu^5 \tag{12}$$

where it is understood that a 5-th order polynomial fitting is employed. Equation (12) defines a key step in the evaluation procedure of the crack growth resistance curve. By measuring the instantaneous compliance during unloading of the specimen (see Fig. 1), the current crack length follows directly from solving the above expression for μ. Table 1 provides the polynomial coefficients of Eq. (12) derived from a standard least square fitting for the pin-loaded and clamped SE(T) specimens. The solid lines displayed in the plots define the fitting curves corresponding to Eq. (12).

Table 1 *Coefficients for the polynomial fitting of Eq. (12).*

		c_0	c_1	c_2	c_3	c_4	c_5
SE(T)$_P$	all *H/W*	1.0056	−2.8744	5.4420	−12.510	16.102	−7.0642
SE(T)$_C$	*H/W*=4	2.3928	−14.074	47.881	−104.58	124.20	−59.423
	H/W=6	2.1263	−13.461	51.299	−120.47	147.83	−71.812
	H/W=10	1.6485	−9.1005	33.025	−78.467	97.344	−47.227

4.2 *J* Estimation Using Eta-Factors

Based upon the plastic work defined by the plastic component of the area under the load *vs. CMOD* curve or the load *vs. LLD* curve (see Fig. 1(b)), the nondimensional η-factors for the analyzed SE(T) specimen with $H/W = 6$ are obtained using the procedure outlined previously. The analyses consider the effect of loading conditions (pin-load *vs.* clamp) and a wide range of hardening properties ($n = 5$, 10, 20) as described by the constitutive law given by Eq. (9).

Figures 4(a-b) provide the η-factors derived from *CMOD* and *LLD* for the pin-loaded SE(T) specimens (hereafter denoted as $\eta_{J,P}^{CMOD}$ and $\eta_{J,P}^{LLD}$) with varying a/W-ratios. Consider first the results displayed in Fig. 4(a). The $\eta_{J,P}^{CMOD}$-values are essentially independent of strain hardening for the entire range of a/W-ratio. Such response provides a particularly interesting result in that factor $\eta_{J,P}^{CMOD}$ for this specimen remains virtually constant with a value of ≈ 1.0. Consider next the results shown in Fig. 4(b). The behavior displayed by the $\eta_{J,P}^{LLD}$-values constrasts rather sharply with the observed response for $\eta_{J,P}^{CMOD}$. While the *eta*-factor based on *LLD* is relatively insensitive to strain hardening in the range $a/W \gtrsim 0.4$, $\eta_{J,P}^{LLD}$ varies

considerably with n for shallower cracks. More importantly, the $\eta_{J,P}^{LLD}$-values depend strongly on a/W-ratio, particularly in the range $a/W \lesssim 0.4$. Here, we also note that the behavior displayed by the plots of Figs. 4(a-b) remains essentially unchanged for other H/W-ratios. Consequently, these numerical results are understood to represent all applicable values of η-factors for pin-load SE(T) specimens having a wide range of crack sizes relative to specimen width.

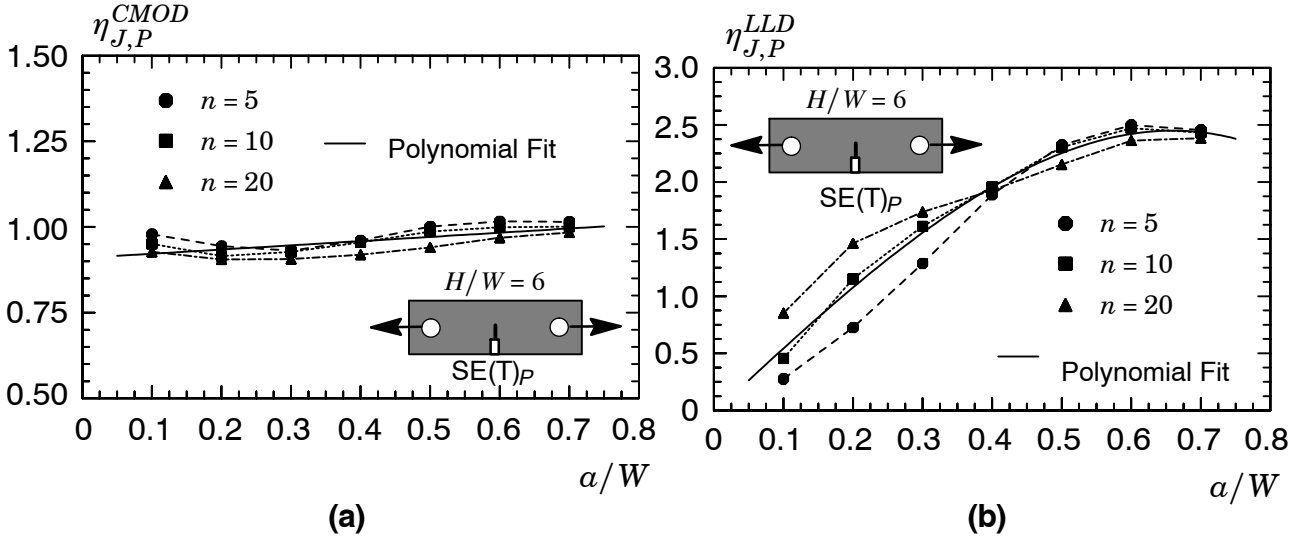

Figure 4 *Variation of plastic η-factor with a/W-ratio for pin-loaded SE(T) specimens: a) derived from CMOD; b) derived from LLD..*

Figure 5 presents the η-factors using *CMOD* for the clamped SE(T) specimens ($\eta_{J,C}^{CMOD}$) with $H/W = 6$ and different a/W-ratios. In contrast to the pin-loaded specimen (see Fig. 4), the $\eta_{J,C}^{CMOD}$-values for this case decrease steadily and almost linearly with crack length in the range $0.10 < a/W < 0.6$. However, the *eta*-factor displays a different trend for $a/W = 0.7$ in which $\eta_{J,C}^{CMOD}$ slightly increases for moderate to low hardening materials ($n = 10$ and 20). Given the very large crack size for this case (which implies a very reduced crack ligament), such behavior may be due to the impingement of the gross bending (and associated in-plane plastic deformation) on the local crack-tip plastic zones thereby affecting the plastic work (upon which factor η is determined). Similar trends are observed for other H/W-ratios. However, the *eta*-factors for these cases also display relatively weak dependence on the H/W-ratio. Since the focus of this work rests primarily on the utilization of pin-loaded SE(T) specimens, those results are omitted to conserve space.

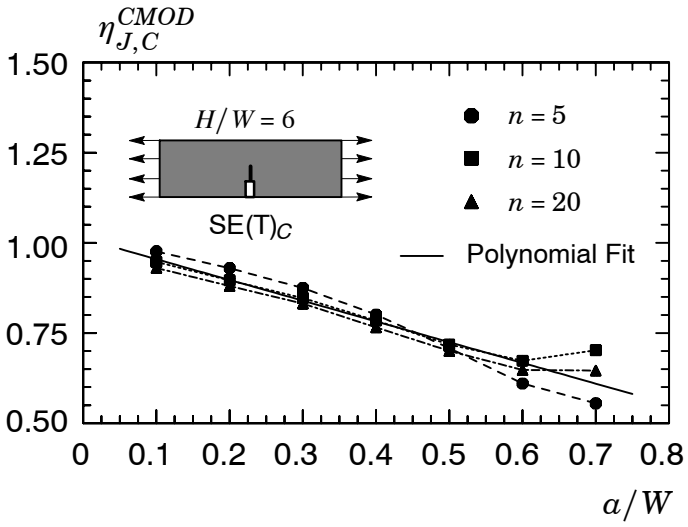

Figure 5 *Variation of plastic η-factor with a/W-ratio derived from CMOD for clamped SE(T) specimens.*

To provide a simpler manipulation of the previous results in evaluation procedures for crack growth resistance curves, the following equations provide a polynomial fit (derived from a standard least square technique) to the dependence of the η-factors on a/W-ratio:

$$\eta_{J,P}^{CMOD} = 0.9095 + 0.1227(a/W) \tag{13}$$

$$\eta_{J,P}^{LLD} = -0.1683 + 7.3828(a/W) - 5.1833(a/W)^2 \tag{14}$$

$$\eta_{J,C}^{CMOD} = 1.0120 - 0.5747(a/W) \tag{15}$$

where it is understood that subscripts P and C refer to pin-loaded and clamped SE(T) specimens. The solid lines in the plots displayed in Figs. (4-5) define the above fitting curves. Further, by taking the derivative of these expressions with respect to the crack size and using Eqs. (6-8), correction of the J-integral for crack growth through Eq. (5) is then readily performed.

5. CONCLUDING REMARKS

This study describes an estimation procedure of crack growth resistance curves for SE(T) fracture specimens using the unloading compliance technique based upon testing of a single specimen. The methodology follows from determining the instantaneous value of the specimen compliance at partial unloading during the experimental measurement of the load-displacement data which enables accurate estimations of J and crack extension, Δa, with increased loading. The extensive plane-strain analyses reported here provide a full set of nondimensional compliance, μ, and plastic factors η and γ for a wide range of specimen geometries, including pin-load and fixed ends, and material properties characteristic of structural, pressure vessel and pipeline steels.

Our results reveal that the compliance μ for the pin-loaded SE(T) specimen is essentially independent of specimen length as characterized by the H/W-ratio. For the clamped SE(T) specimens, however, the compliance μ depends on the H/W-ratio for deeper cracks ($a/W \gtrsim 0.4$), but is essentially independent of specimen length for shallow cracks ($a/W \lesssim 0.2$). The loading condition also affects rather strongly the behavior of the plastic η-factors derived from our analyses. Here, however, specification of the plastic area, A_{pl}, (upon which factor η is based) in terms of CMOD or LLD plays a significant role in defining a more accurate and convenient parameter to determine the J-value with increased crack extension. Our analyses demonstrate that η-factors derived from CMOD are essentially independent of strain hardening (and material properties) and provide values which are less sensitive to the loading level than the corresponding η-factors derived from LLD. Clearly, such results favor the use of η_J^{CMOD} in experimental measurements of crack growth resistance data using SE(T) specimens. While additional experimental studies are needed to build a more extensive body of laboratory data, the results presented here provide a definite basis to support developments of standard test procedures for constraint-designed SE(T) specimens applicable in measurements of crack growth resistance for pipelines.

6. ACKNOWLEDGMENTS

This investigation is supported by Fundação de Amparo à Pesquisa do Estado de São Paulo (FAPESP) through Grant 03/02735-6.

7. REFERENCES

American Welding Society (AWS), 1987, "Welding Handbook: Welding Technology", Eighth Edition, Vol. 1, Miami.
Anderson, T. L., 2005, "Fracture Mechanics: Fundaments and Applications - 3rd Edition", CRC Press, Boca Raton.
API-1104, 1999, "Welding of Pipelines and Related Facilities," 19th Edition, American Petroleum Institute.
ASTM E1820, 2001, "Standard Test Method for Measurement of Fracture Toughness", American Society for Testing and Materials.
Blatt, D., John, R. and Coker, D., 1994, "Stress Intensity Factor and Compliance Solutions for a Single Edge Notched Specimen with Clampd Ends", *Engineering Fracture Mechanics*, Vol. 47, pp. 521-532.
Cravero, S. and Ruggieri, C., 2005, "Correlation of Fracture Behavior in High Pressure Pipelines with Axial Flaws Using Constraint Designed Test Specimens - Part I: Plane-Strain Analyses," *Engineering Fracture Mechanics*, **72**, pp. 1344-1360.
CSA-Z662-99, 1999 , "Oil and Gas Pipeline Systems," Canadian Standards Association.
Eiber, R. J. and Kiefner, J. F., 1986, "Failure of Pipelines", in Metals Handbook, Ninth Edition, Vol. 11 - Failure Analysis and Prevention, American Society for Metals, pp. 695-706.
John, R., 1997, "Stress Intensity Factor and Compliance Solutions for an Eccentrically Loaded Single Edge Cracked Geometry", *Engineering Fracture Mechanics*, Vol. 58, pp. 87-96.

John, R. and Rigling, B., 1998, "Effect of Height to Width Ratio on *K* and CMOD Solutions for a Single Edge Cracked Geometry with Clamped Ends", *Engineering Fracture Mechanics*, Vol. 60, pp. 147-156.
Joyce, J. A., and Link R. E., 1995, "Effects of Constraint on Upper Shelf Fracture Toughness," *Fracture Mechanics, 26th Volume, ASTM STP 1256*, W. G. Reuter, et al. Eds., American Society for Testing and Materials, Philadelphia, pp. 142-177.
Koppenhoefer, K., Gullerud, A., Ruggieri, C., Dodds, R. and Healy, B., 1994, "WARP3D: Dynamic Nonlinear Analysis of Solids Using a Preconditioned Conjugate Gradient Software Architecture," *Structural Research Series (SRS) 596*. UILU-ENG-94-2017. University of Illinois at Urbana-Champaign.
Moran, B., and Shih, C.F., 1987, "A General Treatment of Crack Tip Contour Integrals." *International Journal of Fracture*, **35**, pp.295-310.
National Energy Boarding (NEB), 1996, "Stress Corrosion Cracking on Canadian Oil and Gas Pipelines", Report MH-2-95, Calgary.
Nyhus, B., 1999, "Oseberg Gas Transportation - OGT Repair Welding." *SINTEF Report,* STF24 F99277, Norwegian University of Technology (NTNU).
Nyhus, B. and Ostby, E., 2002, "SENT Testing of High Strength Steel." *in* 2nd International Symposium on High Strength Steel, Verdal, Norway.
Rice, J. R., 1968, "A Path Independent Integral and the Aproximate Analysis of Strain Consentration by Notches and Cracks", *Journal of Applied Mechanics*, **35**, pp. 379-386.
Saxena, A., 1998, "Nonlinear Fracture Mechanics for Engineers", CRC Press, Boca Raton.
Sumpter, J. D. G. and Turner, C. E., 1976, "Method for Laboratory Determination of J_c," Cracks and Fracture, ASTM STP 601, American Society for Testing and Materials, pp 3-18.
Tada, H., Paris, P. C. and Irwin, G. R., 1985, *The Stress Analysis of Cracks Handbook*, 2nd Ed.

10. RESPONSIBILITY NOTICE

The authors are the only responsible for the printed material included in this paper.

APPENDIX:
Stress Intensity Factor Solutions for SE(T) Specimens

Evaluation of the *J*-integral for the SE(T) specimens requires accurate solutions for the (Mode I) elastic stress intensity factor, K_I, appearing in the first term of Eq. (1) or (3) presented in Section 2. While some previous studies (Blatt *et al.*, 1994; John, 1997; John and Rigling, 1998; Tada *et al.*, 1985) provide the stress intensity factors for these crack configurations, these published solutions cover a limited geometry range, particularly a/W and H/W-ratios. The present section provides a comprehensive set of K_I-solutions for pin-loaded and clamped SE(T) fracture specimens with varying specimen geometry (different a/W and H/W-ratios) and eccentricity of loading (offset in the loading point relative to the center of the specimen for the pin-loaded fracture specimen).

The stress intensity factor is conveniently defined in the form

$$K_I = \frac{P}{B\sqrt{W}}\,\mathcal{F}(a/W) \tag{A.1}$$

where $\mathcal{F}(a/W)$ defines a nondimensional stress intensity factor dependent upon specimen geometry, crack size and loading condition. Here, P is the applied load, B denotes the specimen thickness and W is the specimen width. For any given value of P, B and W, calculation of K_I follows from evaluation of $\mathcal{F}(a/W)$ for a given a/W-ratio and loading condition (pin-load or clamp).

An extensive series of linear finite element analyses for pin-loaded and clamped SE(T) analyses was conducted to evaluate the nondimensional stress intensity factor, $\mathcal{F}(a/W)$, for different a/W and H/W-ratios. The analyis matrix (see Fig. 2) includes fracture specimens with crack size in the range $0.1 \le a/W \le 0.7$ with increments of 0.1 and with distance between the pin loading or clamps $H/W = 2, 4, 6, 8, 10, 20$ and 50. The finite element code WARP3D (Koppenhoefer, 1994) provides the numerical solutions for the linear elastic analysis described here. For each model, evaluation of the elastic stress intensity factor follows from computational of the *J*-integral using the conventional relationship $J = K_I^2/E'$ where $E' = E/(1-\nu^2)$ with $\nu = 0.3$ and $E = 206$ GPa in all analyses. The finite element models employed in these computations have essentially similar mesh details as the numerical models previously described in Section 3.

Figure A.1 provides the key results describing the K_I-solutions for the analyzed crack configurations in terms of the variation of the nondimensional stress intensity factor, $\mathcal{F}(a/W)$ with a/W-ratio for different loading conditions, H/W-ratios. The plots displayed in Fig. A.1(a) reveals that the variation of $\mathcal{F}(a/W)$ with a/W-ratio for the pin-loaded specimen remains unchanged for varying H/W-ratios; such results are entirely consistent with the stress intensity solutions for pin-loaded SE(T) specimen given by Tada *et al.* (1985). In contrast, there is a strong effect of the H/W-ratio on $\mathcal{F}(a/W)$ for the clamped specimen shown in Fig. A.1(b), particularly for moderate to deep cracks ($0.3 \le a/W \le 0.7$).

Using again the previous results for guidance, we construct the functional dependence of the nondimensional stress intensity factor and a/W-ratio as follows:

$$\mathcal{F}(a/W) = \xi_0 + \xi_1(a/W) + \xi_2(a/W)^2 + \xi_3(a/W)^3 + \xi_4(a/W)^4 + \xi_5(a/W)^5 \tag{A.2}$$

where it is understood that a 5-th order polyonomial fitting is employed. Table A.1 provides the polynomial coefficients of Eq. (12) derived from a standard least square fitting for the pin-loaded and clamped SE(T) specimens. The solid lines displayed in the plots define the fitting curves corresponding to Eq. (A.2).

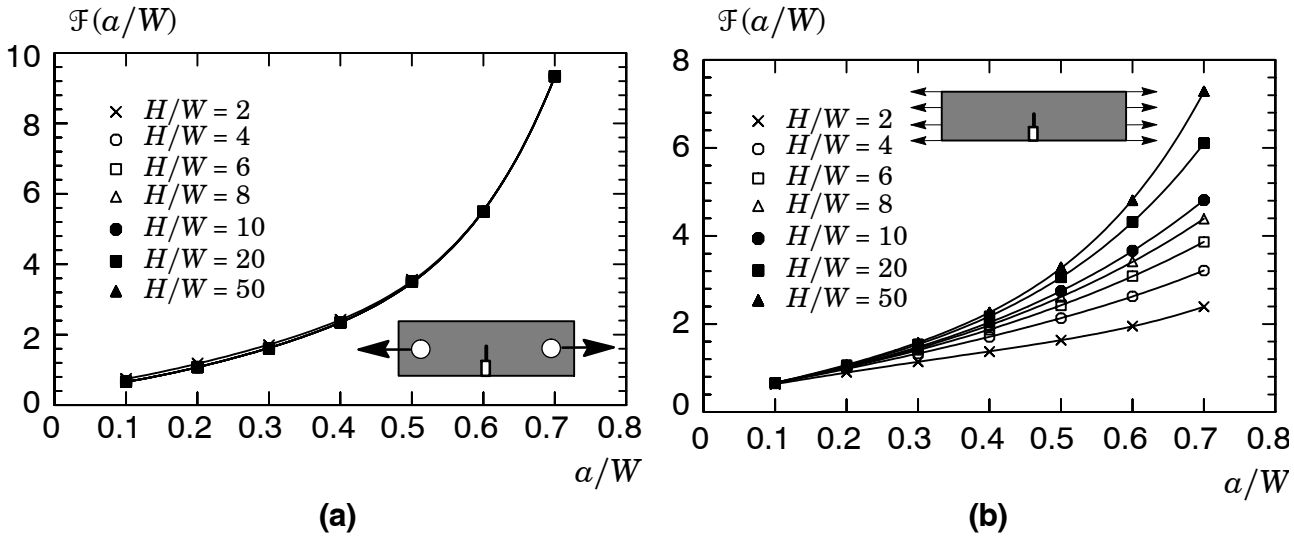

Figure A.1. *Nondimensional stress intensity factor with a / W-ratio: (a) pin-loaded SE(T) specimens; (b) clamped SE(T) specimens.*

Table A.1 Coefficients for the polynomial fitting of Eq. (A.2).

Specimen		ξ_0	ξ_1	ξ_2	ξ_3	ξ_4	ξ_5
$SE(T)_P$	*all H/W*	−0.0720	11.6294	−61.6928	223.4007	−355.5166	239.3969
$SE(T)_C$	*H/W*=2	0.2390	4.7685	−10.8390	22.8483	−25.1329	13.8204
	H/W=4	0.2565	4.4604	−7.0538	18.6928	−19.4703	9.2523
	H/W=6	0.2681	4.1916	−4.5098	12.5442	−6.4726	0.7304
	H/W=8	0.2852	3.8168	−1.4522	3.5078	9.4071	−7.8491
	H/W=10	0.2832	3.8497	−1.4885	4.1716	9.9094	−7.4188
	H/W=20	0.2682	4.1767	−3.8639	14.9622	−7.9416	9.4143
	H/W=50	0.0746	8.2866	−34.2306	117.6196	−165.6966	104.8546